

Self-supervised representation learning from 12-lead ECG data

Temesgen Mehari & Nils Strodthoff

Abstract—We put forward a comprehensive assessment of self-supervised representation learning from short segments of clinical 12-lead electrocardiography (ECG) data. To this end, we explore adaptations of state-of-the-art self-supervised learning algorithms from computer vision (*SimCLR*, *BYOL*, *SwAV*) and speech (*CPC*). In a first step, we learn contrastive representations and evaluate their quality based on linear evaluation performance on a downstream classification task. For the best-performing method, *CPC*, we find linear evaluation performances only 0.8% below supervised performance. In a second step, we analyze the impact of self-supervised pretraining on finetuned ECG classifiers as compared to purely supervised performance and find improvements in downstream performance of more than 1%, label efficiency, as well as an increased robustness against physiological noise. All experiments are carried out exclusively on publicly available datasets, the to-date largest collection used for self-supervised representation learning from ECG data, to foster reproducible research in the field of ECG representation learning.

Index Terms—electrocardiography, time series analysis, deep neural networks

I. INTRODUCTION

The availability of datasets with high-quality labels is an omnipresent challenge in Machine Learning in general, but in medical application in particular, where the labeling process is particularly expensive and clinical ground truth is in many cases hard to define. However, the amount of unlabeled data often exceeds the amount of labeled data by several orders of magnitude, which represents a strong case for (self-supervised) representation learning from unlabeled data. During the past few years, self-supervised learning has made enormous advances in different domains ranging from natural language processing [1] over speech [2] to computer vision [3].

In this work, we investigate self-supervised representation learning in the context of clinical electrocardiography (ECG) data. The ECG is a non-invasive method that allows to assess the general cardiac condition of a patient. It is therefore an important tool for the first-in-line examination for the diagnosis of cardiovascular diseases, which rank among the diseases of

highest mortality [4]. In particular, the (short) 12-lead ECG, which we focus on in this work, is the most commonly used type of ECG with a very broad clinical applicability ranging from primary care centers to intensive care units. Even though the technology underlying the ECG is by now more than 100 years old and it is an extremely common procedure, which is ordered or provided during 5% of the office visits in the US [5], its interpretation is still performed mostly manually with only limited algorithmic support. Here, it is important to recognize that ECG interpretation is in some cases even challenging for cardiologists [6].

There are deep-learning-based ECG interpretation algorithms with exceptionally high performance [7], [8] that have been trained on large closed-source datasets. The sizes of publicly available datasets are smaller by several orders of magnitude, which provides the motivation to see if and how far self-supervised learning techniques can improve the performance of algorithms trained on these datasets. In addition, the question of label quality remains challenging even for the above large-scale datasets. Beyond evaluating different representation learning algorithms in the domain of ECG data, which is an interesting question as such, self-supervised pretraining might also provide benefits for finetuned classifiers on some downstream task, including improved data efficiency, improved quantitative performance, or improved robustness in a general sense as compared to model trained in a purely supervised fashion. In our experimental results, we try to find evidence for these benefits. Our key achievements can be summarized as follows:

- We present a comprehensive assessment of self-supervised representation learning for 12-lead ECG data.
- We adapt and directly compare self-supervised contrastive methods from computer vision (*SimCLR*, *BYOL*, *SWaV*) and speech (*CPC*) and find compelling evidence for the feasibility of learning useful representation from ECG data through self-supervised learning.
- We propose and evaluate several modifications in the *CPC* architecture and training procedure that lead to considerable performance improvements.
- We evaluate different quality aspects of downstream classifiers finetuned from self-supervised models compared to training from scratch and find evidence for improved quantitative performance (given the same downstream training set), improved label efficiency and improved robustness through self-supervised pretraining.

This work was supported by the Bundesministerium für Bildung und Forschung through the BIFOLD - Berlin Institute for the Foundations of Learning and Data (ref. 01IS18025A and ref. 01IS18037A) and 18HLT07 MedaCare. This project 18HLT07 MedaCare has received funding from the EMPIR programme co-financed by the Participating States and from the European Union's Horizon 2020 research and innovation programme. Temesgen Mehari is with Physikalisch Technische Bundesanstalt, Berlin, Germany and Fraunhofer Heinrich Hertz Institute, Berlin, Germany, email: temesgen.mehari@ptb.de. Nils Strodthoff is with Fraunhofer Heinrich Hertz Institute, Berlin, Germany, e-mail: nils.strodthoff@hhi.fraunhofer.de. Corresponding author: Nils Strodthoff. Both authors contributed equally to this work.

II. RELATED WORK

Contrastive methods in computer vision have witnessed tremendous advances in the past few months [3], [9]–[12], which significantly improved the linear evaluation performance on ImageNet and demonstrated the usefulness of the learned features for other computer vision tasks. These methods can be adapted straightforwardly to learning representations from a large number of relatively short time series segments if one interprets the time series record as a one-dimensional multichannel image and adapts transformations appropriate for time series. A second domain, where self-supervised methods for non-discrete data have been implemented successfully is the domain of representation learning speech, where predictive coding methods [2], [13] have been applied to conventional acoustic features [13]–[15] but also to raw waveform data [2], [16], [17].

Self-supervised methods have also been used for representation learning from biomedical sequence data, including, most prominently, ECG [18]–[21] and electroencephalography (EEG) [18], [19], [22], [23] data. With the exception of [21], none of the existing works considered the case of representation learning from clinical 12-lead ECGs, the clinically most widely encountered type of ECG measurement. The authors of [21] also consider BYOL and SimCLR for pretraining but used a very shallow network architecture with only five layers. We believe that it is necessary to use larger models, which reach state-of-the-art performance on large, comprehensive ECG datasets such as PTB-XL and which consequently allow to learn richer representations, along with pretraining on larger datasets.. In addition, they propose new contrastive methods that can use 12-lead ECG data during pretraining but differ from our methods in that they are not expedient for downstream 12-lead ECG tasks. This is because the proposed models do not process 12-lead data directly but exploit the fact that different leads from the same patient during pretraining can be considered as positive pairs.

From the methodological point of view, [19] is also close to our contrastive approach but their experimental results were limited to a small 2-lead dataset with less than 50 records. Without access to the original implementation, it is impossible to assess if their proposed approach would be competitive on 12-lead data and on large (pretraining) datasets, where self-supervised methods reveal their full potential. Earlier approaches such as [18] trained representations from 2-lead ECGs using skip-gram models. Finally, [20] use transformation recognition as a pretext task and proposed a framework specific to representation learning from single-lead ECGs.

III. METHODS

A. Contrastive methods from computer vision (SimCLR/BYOL/SwAV)

Current state-of-the-art contrastive methods from computer vision aim to learn representations based on multiple views on the same instance. These are created by applying stochastic transformations to the input data. This idea is implemented in the most straightforward way in *SimCLR* [3], where a noise

contrastive loss is used to attract two (positive) copies originating from the same original instance and to repel instances from all other (negative) instances in the batch, an approach which typically relies on training with large batch sizes, which is less problematic in our case due to the reduced dimensionality of time series data as compared to image data. *BYOL* [11] does not explicitly rely on contrasting against negative samples in the same batch, but uses a moving average of the model itself and reported slight improvements over *SimCLR* in the image domain. Finally, *SwAV* [12] relies on contrasting cluster assignments rather than individual instances and once again improved the linear evaluation scores on ImageNet. In our case, we build on the implementations of all three frameworks in *PyTorch Lightning Bolts* [24].

As model architecture, we use the convolutional neural networks of the *xresnet1d*-family, one-dimensional adaptations of the popular *xresnet*-architecture [25] from computer vision, which showed very good performance in a recent ECG classification benchmarking study [26]. For analogy with representation learning in computer vision, where results are conventionally reported for a *resnet50*-architecture, we base our experiments on the *xresnet1d50*-architecture.

The transformations used to generate two semantically equivalent views of a given original record lie at the heart of the recent success of contrastive methods in computer vision. As demonstrated in [3], the quality of the learned representations depends crucially on the choice and proper combination of transformations. We therefore evaluated a number of transformations from transformations inspired by effective transformations in computer vision and transformations specific for time series, see Appendix A for a detailed description. Finally, we also evaluate representations obtained by using only prototypical physiological noise during pretraining.

B. Contrastive methods from speech (CPC)

Contrastive Predictive Coding (*CPC*) [2] is also a contrastive approach, which, in contradistinction to the approaches described above, explicitly makes use of the sequential ordering of the data. The idea is to encode the input sequence by means of an encoder with strided convolutions or fully connected layers and train a model to predict the latent representation of the sequence a fixed number of steps in the future given the encoded representation of the sequence in the past again using a noise contrastive estimation approach. As we work with data at 100 Hz, which is sampled rather coarsely compared typical sampling rates of 10 kHz in the audio domain, there is no need to drastically downsample the signal by means of strided convolutions. Instead, we use a fully connected encoder, in our case composed of four layers with 512 filters with batch normalization, as it was also done in self-supervised representation learning from classical audio features [13]–[15]. We predict 12 steps into the future and work with 128 false negatives that are drawn from the same sequence as the original record. For the prediction task we use a LSTM model [27] with 2 layers and 512 hidden units. We propose and evaluate an enhanced version of the *CPC*

architecture, with an additional hidden layer and non-linearity before the linear output layer of the LSTM. This modification was inspired by the MLP in *SimCLR*, which was one of the key components that lead to superior performance compared to previously used self-supervised approaches in computer vision.

When finetuning a classification model, we apply a concat-pooling layer [28], which concatenates the maximum of all LSTM outputs, the mean of all LSTM outputs, and the LSTM output corresponding to the final step, and a fully connected classification head with a single hidden layer with 512 units including batch normalization and dropout for regularization. To assess linear evaluation performance, we use a single fully connected layer on top of the concat-pooling layer.

IV. EXPERIMENTAL SETUP

A. Datasets

We use a collection of three datasets for pretraining henceforth referred to as *All*, namely *CinC* [29], *Ribeiro* [8] and *Zheng* [30], which constitute a collection of the largest publicly available 12-lead ECG datasets with in total 54,566 records. It is worth mentioning that *CinC*, the training dataset used for the Computing in Cardiology Challenge 2020, is by itself a compilation of five different datasets. In particular, it includes the *PTB-XL* dataset [31], [32] that we also use for evaluation in this study. At the most finegrained level, which is used here, the dataset comes with 71 labels and the evaluation task is framed as a multi-label classification task. It is worthwhile stressing that these labels cover a wide variety of diagnostic, form and rhythm statements and can be used for a comprehensive evaluation of ECG analysis algorithms. The dataset is organized into ten stratified, label-balanced folds, where the first eight are used as training set, the ninth is used as validation set and the tenth fold serves as test set. All datasets are summarized in Table I.

Table I: Dataset Summary: For pretraining we use *All* (*CinC* and *Zheng* and *Ribeiro*) or *PTB-XL*. We evaluate on *PTB-XL*. Note that *PTB-XL* is a subset of *CinC*.

dataset	#samples	# patients
Pretraining: <i>All</i>	54,566	unknown
- <i>CinC</i>	43,093	unknown
- <i>Zheng</i>	10,646	10,646
- <i>Ribeiro</i>	827	827
Evaluation	21,837	18,885
- <i>PTB-XL</i>	21,837	18,885

B. Training and Evaluation Protocol

We restrict ourselves to ECG data at a sampling rate of 100Hz in all cases. We pretrain CPC models on input sequences of length 10 seconds, all other models (including finetuned CPC models) are trained on input sequences of length 2.5 seconds. During training, subsequences are randomly cropped from the input record. During test time while finetuning, we use test-time-augmentation and crop all

non-overlapping sequences of length 2.5 seconds from the original record and take the mean of their respective output probabilities as final prediction, a method which considerably improved the model performance by approximately 0.01 in macro AUC as compared to a naive evaluation [26]. In all cases, we use the AdamW optimizer [33] with a weight decay of 0.001 and a constant learning rate schedule. During pretraining, we optimize the InfoNCE loss [2] for CPC and the respective contrastive loss for *SimCLR*, *BYOL*, and *SwAV* as described in the original publications. During finetuning, we optimize binary crossentropy as appropriate for a multi-label classification task and evaluate the model performance based on macro AUC as in [26], computed from the 71 labels on the most finegrained level in *PTB-XL* [31]. The model selection is performed on the validation set. We select the model with the lowest validation loss during pretraining and highest macro AUC during finetuning, and report its respective test set score.

As conventionally done in self-supervised representation learning studies, we use two different evaluation procedures, *linear evaluation* and *finetuning*. The *linear evaluation* protocol aims to assess the quality of the learned representations through the linear separability of the learned representations. To this end, we replace the classification head by a single linear layer and freeze all other layers as well as batch normalization statistics. Within the *finetuning* protocol, we investigate the usefulness of these representations for downstream tasks, where we unfreeze the classification head as well as all layers of the pretrained model. For *CPC*, we found it beneficial to follow a two-step approach during finetuning: In a first step, we finetune just the classification head while keeping the remaining pretrained weights fixed but still updating batch norm statistics. We perform model selection using validation set scores and then finetune the entire model at a reduced learning rate using discriminative, i.e. layer-dependent learning rates to mitigate the danger of overwriting the information captured during pretraining, where we typically divide models into head, body and stem/encoder and reduce the learning rate by a factor of 10 compared to the respective previous layer group. Also in this case, we select the final model based on validation set scores.

V. EXPERIMENTS

A. *SimCLR*, *BYOL*, and *SwAV* and augmentation transformations

The choice of appropriate transformations to induce two semantically equivalent views on the original instance is crucial for the effectiveness of the approach and one of the key components for the success of *SimCLR* [3]. In order to find the best combination of transformations during pretraining, we followed the example of [3] and performed a grid search, based on six transformations, which are partly inspired from computer vision and partly from time series analysis: *Gaussian noise* (*GN*), *Gaussian blur* (*GB*), *channel resize* (*CR*), *time out* (*TO*), *random resized crop* (*RRC*) and *dynamic time warp* (*DTW*), see Appendix A for a detailed description. For all pairs as well as single transformations, we trained a *xresnet1d50* using *SimCLR* for 500 epochs on the

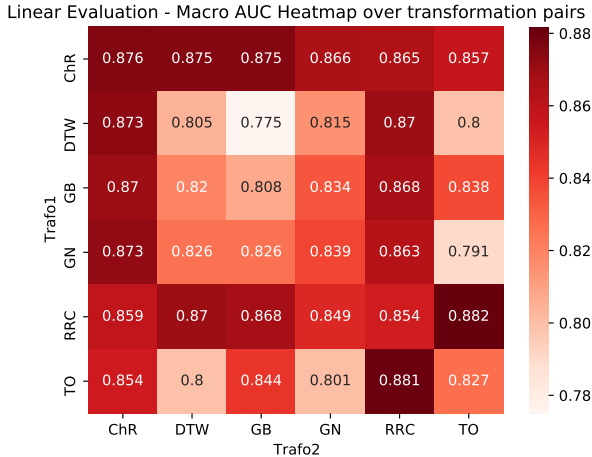


Figure 1: Linear evaluation performance (macro AUC) on the *PTB-XL* validation set of a *xresnet1d50* model after 500 epochs pretraining on *All* with *SimCLR* using one or two data augmentations. Diagonal entries correspond to a single transformation and off-diagonal entries correspond to the sequential composition of two transformations. We report the mean over three linear evaluation runs.

Table II: Comparing different contrastive learning frameworks and augmentation transformations in terms of linear evaluation and finetuning performance after 2000 epochs pretraining on the *All* dataset. We report mean and standard deviation of the validation set scores over 10 finetuning runs using a concise error notation where e.g. 0.8976(11) signifies 0.8976 ± 0.0011 .

method	transformations	PTB-XL	
		lin. eval.	finetuned
SimCLR	(RRC, TO)	0.8976(11)	0.9294(14)
SimCLR	physio.	0.7957(23)	0.9290(13)
BYOL	(RRC, TO)	0.8781(24)	0.9327(20)
BYOL	physio.	0.8483(24)	0.9289(20)
SwAV	(RRC, TO)	0.8227(11)	0.9227(19)
SwAV	physio.	0.7157(27)	0.9260(28)

All dataset. Figure 1 shows the respective linear evaluation performances on the *PTB-XL* dataset. The results rather clearly identify *time out* in combination with *random resized crop* as most effective transformation pair. This is one combination of transformation that will be used for all following experiments. For comparison, we train a model on transformations that are supposed to mimic common types of physiological noise that typically occur in ECG measurements [34], [35]. Here, we consider *baseline wander*, *powerline noise*, *electromyographic noise* and *baseline shift*, which are also described in detail in Appendix A.

In a second step, we aim to identify the most effective pretraining framework. To this end, we pretrain models using *SimCLR*, *BYOL*, and *SwAV* each with (RRC, TO) and physiological noise transformations. The results are summarized in Table II both in terms of linear evaluation as well as finetuned performance. As first observation, in terms of both evaluation

modes the models pretrained with artificial transformations are considerably stronger than their counterparts pretrained using physiological noise. In terms of linear evaluation performance, the gap is smallest in case of *BYOL*, which is consistent with findings about a less pronounced sensitivity to transformation choices in computer vision [11]. However, the most interesting observation is the mismatch between linear evaluation and finetuned model scores: Whereas *SimCLR* reaches clearly the best evaluation performance, finetuning from a *BYOL* representation leads to a superior downstream performance after finetuning. This iterates the fact that the ranking in terms of linear evaluation performance is not necessarily a perfect proxy for the ranking in terms of downstream performance.

B. Self-supervised pretraining learns meaningful representations from ECG data

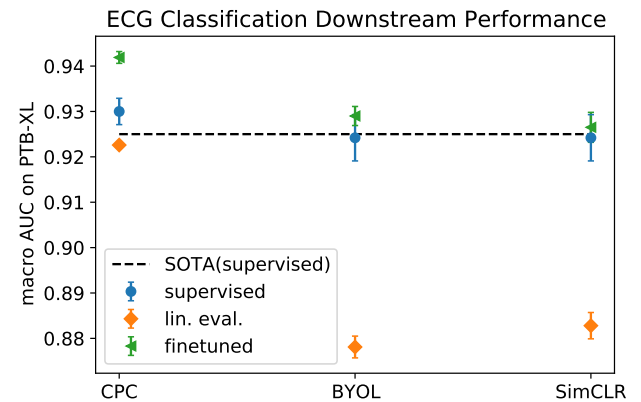


Figure 2: Comparison of different contrastive learning frameworks in terms of downstream performance comparing the three self-supervised learning frameworks *CPC*, *BYOL* and *SimCLR*. The previous supervised state-of-the-art result from [26] is represented by a dashed line.

We start by discussing the linear evaluation performance in Table III, which should be set in perspective to the supervised performance achieved on *PTB-XL*. The best published result for this task on the same dataset with identical splits using purely supervised training was 0.925(07), also using a *xresnet1d*-model [26]. Our supervised results remain slightly below this baseline results, which was, however, also achieved with a deeper *xresnet1d101*-model. The architecture used for *CPC* pretraining (denoted by *4FC+2LSTM+2FC*) was not investigated in previous studies [26] and shows the strongest supervised performance reported on *PTB-XL* thus far.

The linear evaluation performances in Table III show that the pretrained representations are highly relevant for downstream classification tasks. Most notably, the linear evaluation performance of the *CPC* model only shows a performance gap of 0.8% compared to the same model architecture trained in a supervised manner. The contrastive methods from computer vision show a slightly weaker performance, but still the best linear evaluation performance reaches 95.5% of the respective supervised performance. Based on these results, it is justified

Table III: Linear evaluation and finetuning performance on a downstream ECG classification task (macro AUC on the *PTB-XL* test set). As before, we report mean and standard deviation over 10 finetuning runs.

method	model	<i>PTB-XL</i>	
		lin. eval.	finetuned
supervised	4FC+2LSTM+2FC	0.7110(65)	0.9300(29)
supervised	xresnet1d50	0.7210(158)	0.9242(51)
CPC (on All)	4FC+2LSTM+2FC	0.9226(05)	0.9419(13)
CPC (on <i>PTB-XL</i>)	4FC+2LSTM+2FC	0.9204(10)	0.9398(13)
SimCLR (RRC, TO)	xresnet1d50	0.8828(29)	0.9265(33)
SimCLR physio.	xresnet1d50	0.7701(31)	0.9258(13)
BYOL (RRC,TO)	xresnet1d50	0.8781(24)	0.9290(21)
BYOL physio.	xresnet1d50	0.8295(27)	0.9260(25)

to claim that self-supervised representation learning is very effective in the ECG domain. To demonstrate the impact of dataset size, we also report results for pretraining *CPC* just on *PTB-XL* i.e. using only 40% of the original training dataset. As expected, increasing the size of the training dataset leads to improvements in the linear evaluation performance.

C. Self-supervised pretraining improves downstream performance

In this section, we investigate whether finetuning from self-supervised representations can potentially also lead to improvements in downstream performance as compared to purely supervised training. The results are compiled in Table III and summarized graphically in Figure 2. As before, *SimCLR* reaches the best linear evaluation performance whereas it is slightly outperformed by *BYOL* in terms of downstream performance. The considerably better linear evaluation performance of the *CPC* model as compared to *BYOL* and *SimCLR* directly translates into an improved downstream performance. Interestingly, the *SimCLR* and *BYOL* finetuned model performance when using physiological noise during training almost reaches the results from using (RRC,TO)-transformations, while a sizable performance gap exists between them in terms of linear evaluation performance. In all cases, the results from finetuning pretrained models improve over the corresponding supervised results (by 1.3% for *CPC*, by 0.2% for *SimCLR*, and by 0.5% for *BYOL*). Furthermore, it is noticeable that already after the first finetuning step, where just the batch norm statistics and the classification head are adjusted, the *CPC* model reaches performance values around 0.931 i.e. already slightly exceeds supervised performance. These results provide a clear case for self-supervised learning in the ECG domain.

As a final remark, one has to consider the different sizes of models under consideration. Whereas the *CPC*-model during finetuning comprises 5.8M parameters, the *xresnet1d50* only counts 930K parameters, which might suggest the a part of the gap between *CPC* and *BYOL/SimCLR* can at least partially be attributed to a difference in model capacity. However, in preliminary experiments we saw no indications of strong performance increases with wider or deeper models. It remains to see how the performance of *SimCLR* and *BYOL* scales on larger datasets. A serious disadvantage of *CPC* is the sequential nature of the LSTM, which leads to slow training

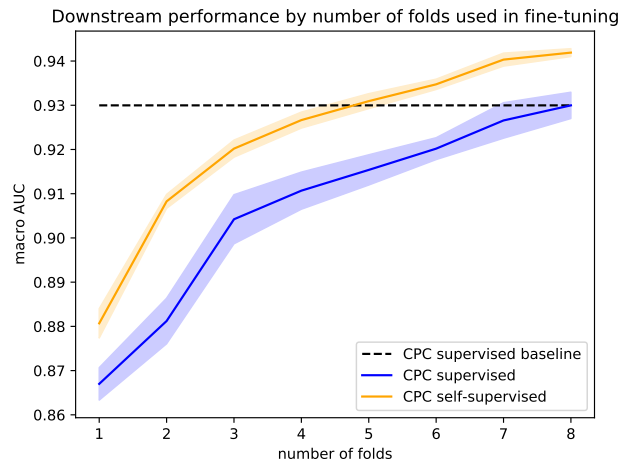


Figure 3: Finetuning downstream performance on *PTB-XL* dataset of a *4FC+2LSTM+2FC*-model pretrained using *CPC* compared to its supervised counterpart. The finetuning was performed for different supervised number of training folds, ranging from 1-8 folds. We used 10 runs for 8 folds as before and 3 runs for 7 folds or fewer. The plot shows the mean performance as a solid line and one standard deviation around it as a shaded band. To guide the eye, we indicate the supervised model performance on the full training set by a dashed line.

times. The training times are not directly comparable due to the different nature of the tasks, but give at least a hint. *CPC* models were pretrained for 200 epochs, which took approximately 6 days on a single Tesla V100 GPU. *SimCLR* and *BYOL* pretraining was performed for 2000 epochs using batch sizes of 8192 with approximate runtimes of 15h and 13h on a single Tesla V100 GPU, respectively. Performing 50+20(100) epochs of finetuning for the *4FC+2LSTM+2FC(xresnet1d50)*-model takes approximately 25(10) minutes on the mentioned hardware.

D. Self-supervised pretraining improves downstream data efficiency

Another potential advantage of self-supervised pretraining lies in a potentially improved data efficiency when finetuned on a downstream task. This is a particularly relevant case for medical applications, where high-quality labels are hard

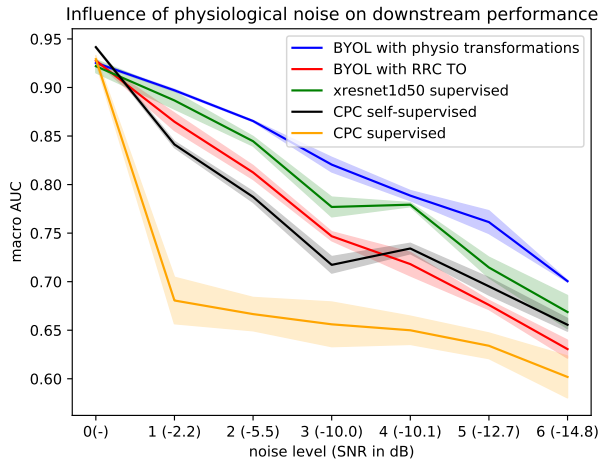


Figure 4: Evaluating the impact of noise on pretrained and purely supervised trained classifiers. We induced typical physiological noise at different strength levels to the test set.

to obtain. To investigate this claim in detail, we compare the performance of different pretrained models from self-supervised representations to models trained from scratch in purely supervised fashion while varying the number of training folds from the original 8 folds to a single fold. This can be read off for example from the number of training folds where the pretrained model reaches the same performance as the supervised model trained on the full dataset. In the case of *CPC*, this point is reached approximately at 5 folds or equivalently approximately 62% of the training data. The performance level of the supervised models at 4 folds is approximately reached by the pretrained model trained only on two folds i.e. 50% of the training data. For *BYOL* and *SimCLR*, the effect is still present but much less pronounced due to the closer proximity of the pretrained and the purely supervised results on the full training set. Figure 3 illustrates nicely illustrates another advantage of self-supervised pretraining, namely the performance across different training runs is much more stable compared to purely supervised training, as visible from considerably reduced error bands, most crucially influenced by the two-step finetuning procedure in combination with discriminative learning rates, see also Section V-F.

E. Self-supervised pretraining improves robustness of downstream classifiers

In addition to quantitative performance and data efficiency, robustness is one of the key quality criteria for machine learning models. Here, we focus on robustness against input perturbations. It is well known that certain types of noise tend to occur in ECG data as a consequence of the measurement process and physiological interference [34], [35]. In Appendix A, we briefly review typical kinds of ECG noise and propose simple ways of parameterizing them. For simplicity, we just superimpose the different noise types and the original ECG waveform. We define different noise levels by adjusting the amplitudes of these noise transformations and

evaluate the performance of the models from the previous sections on perturbed versions of the original test set. We also indicate signal-to-noise-ratios (SNRs) corresponding to the different noise levels, where we identify the signal with the original ECG waveform. However, one has to keep in mind that this assessment neglects the noise inherent in the original measurement, which implies that the given SNRs only upper-bound the actual values.

The goal is to investigate if pretrained models are less susceptible to physiological noise. The results in Figure 4 reveal an interesting pattern: For the *4FC+2LSTM+2FC*-models, the *CPC*-pretrained model shows a considerably improved robustness to noise compared to its supervised counterpart. However, both models turn out to be less robust than the considerably less complex *xresnet1d*-models. For the latter, the *BYOL*-pretrained models with physiological noise shows the strongest overall performance and also performs considerably stronger than the corresponding supervised model. This result provides a strong argument for pretraining with domain-specific noise transformations even if it comes at the cost of a slight performance during noiseless evaluation, see Table III. Somewhat surprisingly, the *BYOL*-pretraining with the artificial (RRC,TO)-transformation even lead to a reduced robustness compared to the supervised *xresnet1d50*. As a final remark, the noise levels 3 and beyond are already strongly dominated by noise and correspond to situations that will rarely be encountered in real-world scenarios.

F. CPC ablation studies

In this final section, we investigate the impact of different modifications of the *CPC* architecture and training procedure to demonstrate in how far they positively impacted the performance. These results potentially convey general insights for *CPC* and related self-supervised approaches that go beyond the specific application to ECG data. Therefore, we vary one aspect while keeping the other ones fixed and report the impact on linear evaluation and finetuning procedure. Pretraining and evaluation is performed on PTB-XL for simplicity. We refer to the configuration with fully connected encoder, MLP during pretraining, predicting 12 steps ahead, hidden layer, batch normalization and dropout in the classification head, two-step finetuning, discriminative learning rates during finetuning as *CPC Baseline*.

Table IV: Impact of different architectural and procedural components during *CPC* pretraining and finetuning. We report the performance in comparison to our baseline result when omitting a specified component.

component	PTB-XL	
	lin. eval.	finetuned
<i>CPC Baseline</i>	0.9226(05)	0.9419(13)
pretraining: no MLP	0.9193(08)	0.9401(13)
head: no hidden layer	-	0.9396(09)
head: no BN nor dropout	-	0.9415(11)
finetuning: no two-step	-	0.9230(21)
finetuning: no discr. lrs	-	0.9419(21)

The results of this investigation are summarized in Table IV: The MLP during *CPC* pretraining has a small but consistent positive impact both in terms of linear evaluation as well on the downstream. Also modifications of the classification head have slight but consistent positive effects. The most significant performance gain arises from finetuning in a two-step approach, where the head is finetuned first and the full model is only finetuned in a second step. Omitting discriminative learning rates in the final pretraining step lead to an identical mean performance as in the baseline case omitted, but the results are much less consistent across different runs as visible from a standard deviation that is almost double the size of the baseline value.

Finally, a comparison to *CPC* applied to raw audio is in order. The original *CPC* [2] applied to raw audio waveforms works on 10 kHz. The encoder uses strided convolutions and the encoded data therefore undergoes a downsampling by a factor of 160. Predicting 12 steps into the future then corresponds to a look-ahead interval of 0.192s. In our case, we work with much more coarsely sampled data at 100 Hz, but the encoded data undergoes no downsampling due to the use of a fully connected encoder. In this case, predicting 12 steps into the future corresponding to 0.120s, which lies in a similar order of magnitude as in speech. Using an encoder with strided convolutions lead to considerably worse performance that was already apparent at the level of the supervised level.

VI. SUMMARY AND CONCLUSIONS

In this work, we put forward a comprehensive assessment of self-supervised representation learning on 12-lead clinical ECG data. Time series represent an interesting application domain that is situated at the intersection of the well-developed domains computer vision and speech processing. However, most of the common datasets in the field are comparably small and the time series often univariate. ECG data is a notable exception in this respect with several recently published public datasets.

Self-supervised learning turns out to be very effective in the ECG domain: Adaptations of self-supervised algorithms from computer vision and speech evaluated under a linear evaluation protocol reach scores that only fall behind 4.5% (*SimCLR*, as best-performing adaptation from computer vision) or even just 0.8% (*CPC*) compared to the respective supervised performances. When finetuning classifiers starting from these pretrained representations, we find performance improvements of 0.5% (*BYOL*) or 1.3% (*CPC*) compared to the performance of their identical counterparts trained in a purely supervised fashion. The sizable performance gap in the case of *CPC* directly translates into an improved label efficiency, i.e. the pretrained model reaches the same performance as the supervised model but using only roughly 50-60% of the samples. As example for a quality dimension beyond quantitative accuracy, we investigate the impact of self-supervised pretraining on the robustness of the corresponding finetuned classifiers against physiological noise. We find increased robustness for most pretrained models compared to the corresponding models trained from scratch, but particularly

for those that were pretrained using domain-specific noise transformations. This provides a strong case for the use of domain-specific noise transformations during pretraining.

To summarize, self-supervised representation learning represents an exciting application domain and already in this first quantitative assessment demonstrated several advantages over purely supervised training. We stress again the free availability of the underlying datasets as an invitation for the self-supervised representation learning community. The source code underlying our study is available [36].

REFERENCES

- [1] J. Devlin, M.-W. Chang, K. Lee, and K. Toutanova, "BERT: Pre-training of deep bidirectional transformers for language understanding," in *Proceedings of the 2019 Conference of the North American Chapter of the Association for Computational Linguistics: Human Language Technologies, Volume 1 (Long and Short Papers)*. Minneapolis, Minnesota: Association for Computational Linguistics, Jun. 2019, pp. 4171–4186.
- [2] A. van den Oord, Y. Li, and O. Vinyals, "Representation learning with contrastive predictive coding," *arXiv preprint 1807.03748*, 2018.
- [3] T. Chen, S. Kornblith, M. Norouzi, and G. Hinton, "A simple framework for contrastive learning of visual representations," in *International Conference on Machine Learning*, 2020.
- [4] E. Wilkins, L. Wilson, K. Wickramasinghe, P. Bhatnagar, J. Leal, R. Luengo-Fernandez, R. Burns, M. Rayner, and N. Townsend, *European Cardiovascular Disease Statistics 2017*. Belgium: European Heart Network, 2 2017.
- [5] CDC, "National Ambulatory Medical Care Survey: 2016 National Summary Tables," Centers for Disease Control and Prevention, Tech. Rep., 2019.
- [6] S. M. Salerno, P. C. Alguire, and H. S. Waxman, "Competency in interpretation of 12-lead electrocardiograms: A summary and appraisal of published evidence," *Annals of Internal Medicine*, vol. 138, no. 9, p. 751, May 2003.
- [7] A. H. Kashou, W.-Y. Ko, Z. I. Attia, M. S. Cohen, P. A. Friedman, and P. A. Noseworthy, "A comprehensive artificial intelligence-enabled electrocardiogram interpretation program," *Cardiovascular Digital Health Journal*, vol. 1, no. 2, pp. 62–70, Sep. 2020.
- [8] A. H. Ribeiro, M. H. Ribeiro, G. M. M. Paixão, D. M. Oliveira, P. R. Gomes, J. A. Canazart, M. P. S. Ferreira, C. R. Andersson, P. W. Macfarlane, W. Meira, T. B. Schön, and A. L. P. Ribeiro, "Automatic diagnosis of the 12-lead ECG using a deep neural network," *Nature Communications*, vol. 11, no. 1, Apr. 2020.
- [9] K. He, H. Fan, Y. Wu, S. Xie, and R. Girshick, "Momentum contrast for unsupervised visual representation learning," in *Proceedings of the IEEE/CVF Conference on Computer Vision and Pattern Recognition*, 2020, pp. 9729–9738.
- [10] X. Chen, H. Fan, R. Girshick, and K. He, "Improved baselines with momentum contrastive learning," *arXiv preprint 2003.04297*, 2020.
- [11] J.-B. Grill, F. Strub, F. Altché, C. Tallec, P. H. Richemond, E. Buchatskaya, C. Doersch, B. A. Pires, Z. D. Guo, M. G. Azar, B. Piot, K. Kavukcuoglu, R. Munos, and M. Valko, "Bootstrap your own latent: A new approach to self-supervised learning," in *Advances in Neural Information Processing Systems*, 2020.
- [12] M. Caron, I. Misra, J. Mairal, P. Goyal, P. Bojanowski, and A. Joulin, "Unsupervised learning of visual features by contrasting cluster assignments," in *Advances in Neural Information Processing Systems*, 2020.
- [13] Y.-A. Chung, W.-N. Hsu, H. Tang, and J. Glass, "An unsupervised autoregressive model for speech representation learning," *Proc. Interspeech 2019*, pp. 146–150, 2019.
- [14] M. A. C. Blandón and O. Räsänen, "Analysis of predictive coding models for phonemic representation learning in small datasets," *ICML Workshop on Self-supervision in Audio and Speech*, 2020.
- [15] L. van Staden and H. Kamper, "A comparison of self-supervised speech representations as input features for unsupervised acoustic word embeddings," *arXiv preprint 2012.07387*, 2020.
- [16] S. Schneider, A. Baevski, R. Collobert, and M. Auli, "wav2vec: Unsupervised pre-training for speech recognition," *arXiv preprint 1904.05862*, 2019.
- [17] A. Baevski, H. Zhou, A. Mohamed, and M. Auli, "wav2vec 2.0: A framework for self-supervised learning of speech representations," in *Advances in Neural Information Processing Systems*, 2020.

- [18] Y. Yuan, G. Xun, Q. Suo, K. Jia, and A. Zhang, “Wave2vec: Deep representation learning for clinical temporal data,” *Neurocomputing*, vol. 324, pp. 31–42, Jan. 2019.
- [19] J. Y. Cheng, H. Goh, K. Dogrusoz, O. Tuzel, and E. Azemi, “Subject-aware contrastive learning for biosignals,” *arXiv preprint 2007.04871*, 2020.
- [20] P. Sarkar and A. Etemad, “Self-supervised ECG representation learning for emotion recognition,” *IEEE Transactions on Affective Computing*, pp. 1–1, 2020.
- [21] D. Kiyasseh, T. Zhu, and D. A. Clifton, “Clocs: Contrastive learning of cardiac signals across space, time, and patients,” *arXiv preprint 2005.13249*, 2020.
- [22] H. Banville, I. Albuquerque, A. Hyvarinen, G. Moffat, D.-A. Engemann, and A. Gramfort, “Self-supervised representation learning from electroencephalography signals,” in *2019 IEEE 29th International Workshop on Machine Learning for Signal Processing (MLSP)*. IEEE, Oct. 2019.
- [23] H. Banville, O. Chehab, A. Hyvarinen, D. Engemann, and A. Gramfort, “Uncovering the structure of clinical eeg signals with self-supervised learning,” *Journal of Neural Engineering*, 2020.
- [24] W. Falcon and K. Cho, “A framework for contrastive self-supervised learning and designing a new approach,” *arXiv preprint arXiv:2009.00104*, 2020.
- [25] T. He, Z. Zhang, H. Zhang, Z. Zhang, J. Xie, and M. Li, “Bag of tricks for image classification with convolutional neural networks,” in *Proceedings of the IEEE Conference on Computer Vision and Pattern Recognition*, 2019, pp. 558–567.
- [26] N. Strodthoff, P. Wagner, T. Schaeffter, and W. Samek, “Deep learning for ECG analysis: Benchmarks and insights from PTB-XL,” *IEEE Journal of Biomedical and Health Informatics*, pp. 1–1, 2020.
- [27] S. Hochreiter and J. Schmidhuber, “Long short-term memory,” *Neural computation*, vol. 9, no. 8, pp. 1735–1780, 1997.
- [28] J. Howard and S. Ruder, “Universal language model fine-tuning for text classification,” in *Proceedings of the 56th Annual Meeting of the Association for Computational Linguistics (Volume 1: Long Papers)*. Melbourne, Australia: Association for Computational Linguistics, Jul. 2018, pp. 328–339.
- [29] E. A. P. Alday, A. Gu, A. J. Shah, C. Robichaux, A.-K. I. Wong, C. Liu, F. Liu, A. B. Rad, A. Elola, S. Seyedi, Q. Li, A. Sharma, G. D. Clifford, and M. A. Reyna, “Classification of 12-lead ECGs: the PhysioNet/computing in cardiology challenge 2020,” *Physiological Measurement*, vol. 41, no. 12, p. 124003, Jan. 2021.
- [30] J. Zheng, J. Zhang, S. Danioko, H. Yao, H. Guo, and C. Rakovski, “A 12-lead electrocardiogram database for arrhythmia research covering more than 10, 000 patients,” *Scientific Data*, vol. 7, no. 1, Feb. 2020.
- [31] P. Wagner, N. Strodthoff, R.-D. Boussejot, D. Kreiseler, F. I. Lunze, W. Samek, and T. Schaeffter, “PTB-XL, a large publicly available electrocardiography dataset,” *Scientific Data*, vol. 7, no. 1, p. 154, 2020.
- [32] A. L. Goldberger, L. A. N. Amaral, L. Glass, J. M. Hausdorff, P. C. Ivanov, R. G. Mark, J. E. Mietus, G. B. Moody, C.-K. Peng, and H. E. Stanley, “PhysioBank, PhysioToolkit, and PhysioNet,” *Circulation*, vol. 101, no. 23, pp. e215–e220, 2000.
- [33] I. Loshchilov and F. Hutter, “Decoupled weight decay regularization,” in *International Conference on Learning Representations*, 2019.
- [34] G. Friesen, T. Jannett, M. Jadallah, S. Yates, S. Quint, and H. Nagle, “A comparison of the noise sensitivity of nine QRS detection algorithms,” *IEEE Transactions on Biomedical Engineering*, vol. 37, no. 1, pp. 85–98, 1990.
- [35] G. Lenis, N. Pilia, A. Loewe, W. H. W. Schulze, and O. Dössel, “Comparison of baseline wander removal techniques considering the preservation of ST changes in the ischemic ECG: A simulation study,” *Computational and Mathematical Methods in Medicine*, vol. 2017, pp. 1–13, 2017.
- [36] T. Mehari and N. Strodthoff, 2021. [Online]. Available: <https://github.com/hhi-aml/ecg-selfsupervised>

APPENDIX

In this section, we address the transformations used for the presented computer vision-based self-supervised learning methods (SimCLR, BYOL, SwAV). We distinguish between artificial transformations (Appendix A), which are partially adapted versions of the transformations used in [3] or transformations specific to time series, and physiological transformations (Appendix B), which are more realistic perturbations

that occur due to inaccuracies in the measurement process. Figure 5 and Figure 6 depict single-lead examples for each of the artificial and physiological transformations, respectively.

A. Artificial transformation

a) *Gaussian noise*: *Gaussian noise* describes the addition of zero-mean Gaussian noise to all channels. The standard deviation σ of the noise is the only parameter of the transformation. We used $\sigma = 0.01$ mV in our experiments.

b) *Gaussian blur*: *Gaussian blur* describes the application of a one-dimensional Gaussian kernel k to the ECG signal, which results in a blurred version of the signal. More specifically, We used a kernel with entries $(0.1, 0.2, 0.4, 0.2, 0.1)$ in our experiments.

c) *Channel resize*: *Channel resize* multiplies the i -th channel of the signal by the factor $c_i = b_i^a$, where b is the only parameter of the transformation and a_i is uniformly sampled from $[-1, 1]$, such that $\mathbb{E}[c_i] = 1$. In our experiments we chose $b = 3$. *Channel resize* can be seen as an analogue of color transformations in computer vision.

d) *Random resized crop*: *Random resized crop* crops a random contiguous segment of the signal and rescales it to its original size. We sample the crop parameter p uniformly from the range (l, m) , where (l, m) are the parameters of the transformation. In our experiments we used $(l, m) = (0.5, 1.0)$, that is we cropped the signals to portions between 50%-100%.

e) *Time out*: *Timeout* [19] sets a random contiguous segment of the signal to zero. It accepts as parameters a range (t_l, t_u) , from which the timeout parameter t is uniformly sampled. The parameter describes how much of the signal will be set to zero. In our experiments, we used $(t_l, t_u) = [0.0, 0.5]$, therefore we set up to 50% of the signal to zero.

f) *Dynamic time warp*: *Dynamic time warp* stretches and squeezes random contiguous segments of the signal along the x-axis. The parameters are the number of warps w and the radius r of the warps (in timesteps). We used $w = 3$ and $r = 10$.

B. ECG-specific physiological noise transformations

a) *Baseline wander*: Baseline wander is a low-frequency ECG artifact that arises from respiration, electrically charged electrodes or movement of the patient. Here, we follow [35] and model it as a superposition of different sinusoidal components:

$$n_{\text{blw}}(t)_i = C c_i \sum_{k=1}^K a_k \cos(2\pi t k \Delta f + \phi_k), \quad (1)$$

where C, a_k, ϕ_k are uniform random numbers with ranges $[0, C_{\text{max,blw}}]$, $[0, 1]$, and $[0, 2\pi]$. We use $\Delta f = 0.01$ Hz, $f_c = 0.05$ Hz and $K = \lfloor \Delta f / f_c \rfloor$. c_i , where the index i designates the i th lead, is drawn from a standard normal distribution and modulated by a random sign.

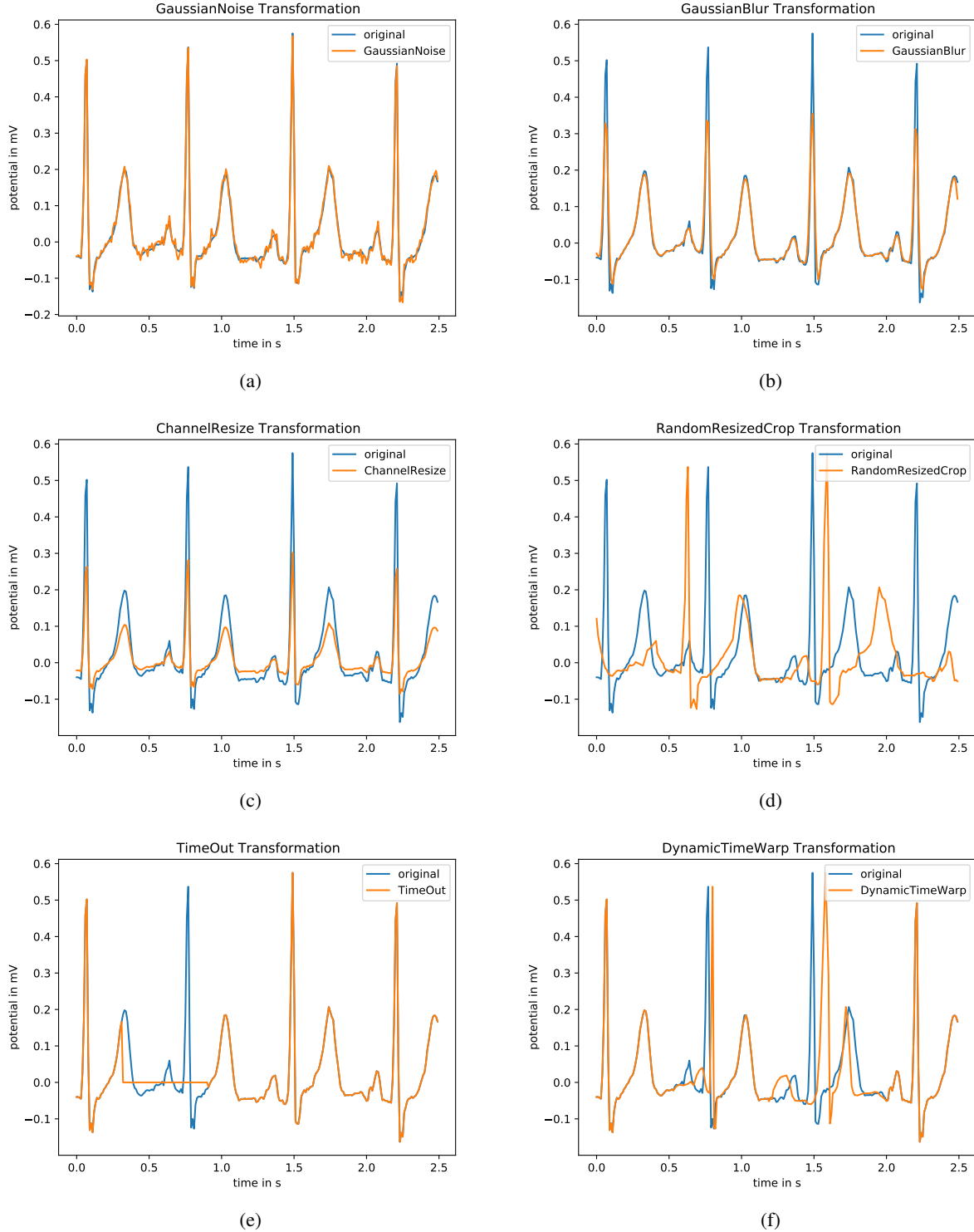


Figure 5: Artificial Transformations used for computer vision based self-supervised methods: (a) *Gaussian noise*, (b) *Gaussian blur*, (c) *Channel resize*, (d) *Random resized crop* and (e) *Time out*.

b) Powerline noise: Powerline noise describes powerline interference pickup at $f_n = 50$ Hz and its higher harmonics [34]. Here, it is modeled as

$$n_{\text{pln}}(t)_i = C c_i \sum_{k=1}^K a_k \cos(2\pi k f_n t + \phi_1), \quad (2)$$

with $K = 3$ and variables as defined above except for c_i , which is drawn from a uniform distribution over $[-1, 1]$ in this case and C , which is a uniform random number drawn from $[0, C_{\text{max,pln}}]$.

c) Electromyographic noise: Electromyographic describes high-frequency noise typically caused by muscle con-

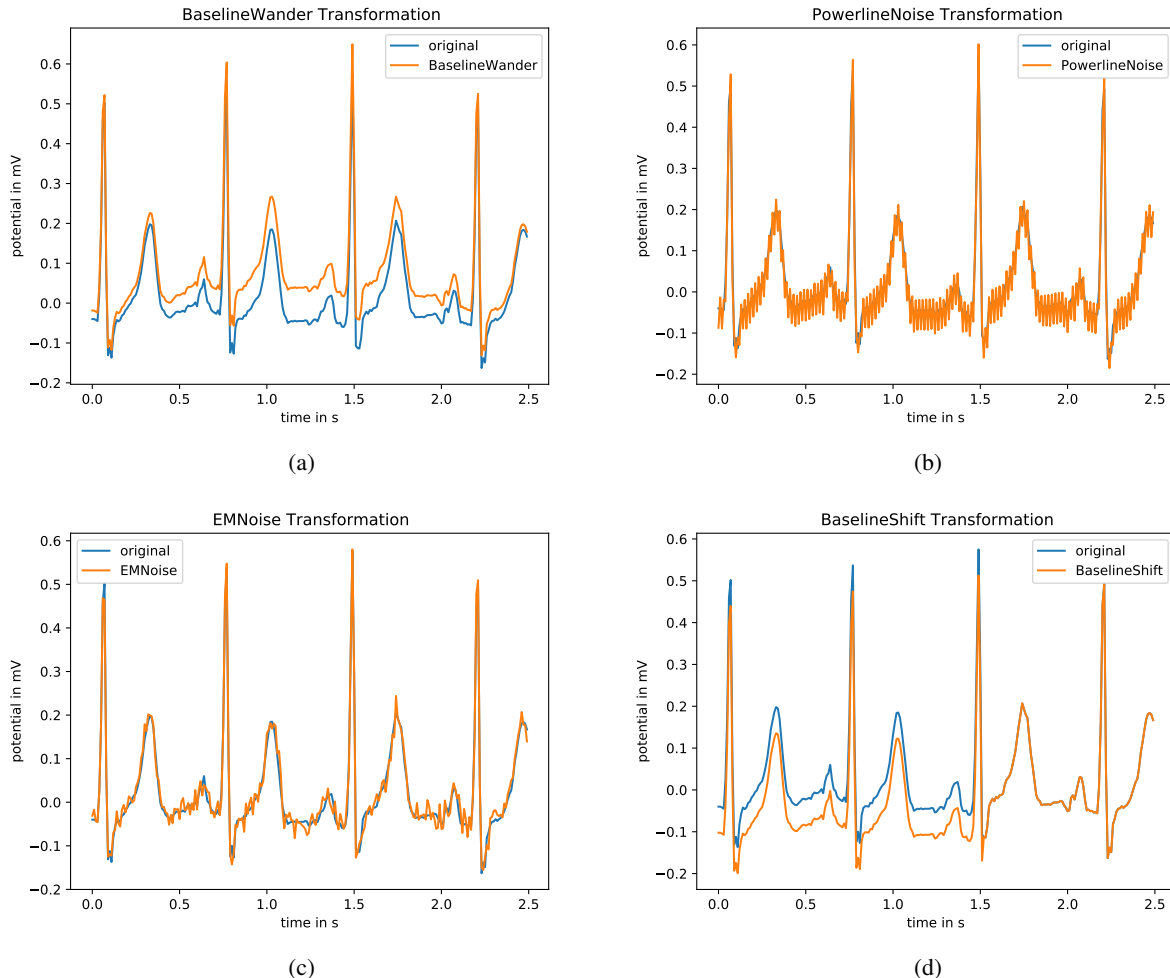


Figure 6: ECG-specific physiological noise transformations used in computer vision based self-supervised methods: (a) *Baseline wander*, (b) *Powerline noise*, (c) *Electromyographic noise* and (d) *Baseline shift*.

Table V: Mapping of noise levels to corresponding parameters of physiological transformations.

noise level	$C_{\max,blw}$	$C_{\max,pln}$	$C_{\max,emn}$	$C_{\max,bls}$	SNR
1	0.05	0.25	0.1	0.5	-2.2
2	0.1	0.5	0.2	1	-5.5
3	0.1	1	0.2	2	-10.0
4	0.2	1	0.4	2	-10.1
5	0.2	1.5	0.4	2.5	-12.7
6	0.3	2	0.5	3	-14.8

transformations [34]. Here, we simply model it as Gaussian noise:

$$n_{emn}(t)_i = \beta, \quad (3)$$

where β is drawn from a normal distribution with mean zero and variance $C_{\max,emn}$.

d) Baseline shift: Baseline shift describes baseline changes through electrode-skin impedance changes through electrode motion [34]. Following [34], we model this type of

noise by sampling a stepwise function $swf(t)$. In our case, it is created as follows: We determine the number of segments by drawing a random integer from $[0, \lceil bls_{\max} * L / f_s \rceil]$, where $bls_{\max} = 0.3s^{-1}$, L is the length of the segment (in timesteps) and f_s is the sampling frequency. For each segment, we add a step function with non-zero values at a segment with length drawn from a normal distribution with mean $f_s bls_{len,mean}$ and standard deviation $0.2f_s bls_{len,mean}$, where $bls_{len,mean} = 3s$. The amplitude of each segment determined in this way is drawn from a random uniform distribution. Given, the sampled stepwise constant function $swf(t)$, one defines the baseline shift noise via

$$n_{bls}(t)_i = Cc_i swf(t), \quad (4)$$

where C is a uniform random number drawn from $[0, C_{\max,bls}]$ and c_i is drawn from a standard normal distribution and modulated by a random sign.

e) Superposition: Eventually, all four noise types are superimposed and added to the original signal $s(t)$ i.e.

$$s_{\text{physio. noise}}(t) = s(t) + n_{blw}(t) + n_{pln}(t) + n_{emn}(t) + n_{bls}(t) \quad (5)$$

The noise strength is adjusted by varying $C_{\max,blw}$, $C_{\max,pln}$, $C_{\max,emn}$, and $C_{\max,bls}$ while keeping all other parameters fixed.

C. Parameter values used during pretraining and evaluation

During pretraining, we used $C_{\max,blw} = 0.1$, $C_{\max,pln} = 0.2$, $C_{\max,emn} = 0.5$, and $C_{\max,bls} = 1$ when using the physiological transformations. For our robustness test, we created noisy validation sets. We considered different levels of noise, which are described in Table V.